



Exploring Poly(Ethylene Glycol)-Poly(Trimethylene Carbonate) Nanoparticles as Carriers of Hydrophobic Drugs to Modulate Osteoblastic Activity

Leite DM¹, Sousa DM², Lamghari M³, Pêgo AP⁴

1 i3S - Instituto de Investigação e Inovação em Saúde, Universidade do Porto, Rua Alfredo Allen, 208, 4200-135 Porto, Portugal; INEB - Instituto de Engenharia Biomédica, Universidade do Porto, Rua Alfredo Allen, 208, 4200-135 Porto, Portugal; FEUP - Faculdade de Engenharia da Universidade do Porto, R. Dr. Roberto Frias s/n, 4200-465 Porto, Portugal.

2 i3S - Instituto de Investigação e Inovação em Saúde, Universidade do Porto, Rua Alfredo Allen, 208, 4200-135 Porto, Portugal; INEB - Instituto de Engenharia Biomédica, Universidade do Porto, Rua Alfredo Allen, 208, 4200-135 Porto, Portugal.

3 i3S - Instituto de Investigação e Inovação em Saúde, Universidade do Porto, Rua Alfredo Allen, 208, 4200-135 Porto, Portugal; INEB - Instituto de Engenharia Biomédica, Universidade do Porto, Rua Alfredo Allen, 208, 4200-135 Porto, Portugal; ICBAS - Instituto de Ciências Biomédicas Abel Salazar, Universidade do Porto, R. de Jorge Viterbo Ferreira, 228, 4050-313 Porto, Portugal.

4 i3S - Instituto de Investigação e Inovação em Saúde, Universidade do Porto, Rua Alfredo Allen, 208, 4200-135 Porto, Portugal; INEB - Instituto de Engenharia Biomédica, Universidade do Porto, Rua Alfredo Allen, 208, 4200-135 Porto, Portugal; FEUP - Faculdade de Engenharia da Universidade do Porto, R. Dr. Roberto Frias s/n, 4200-465 Porto, Portugal; ICBAS - Instituto de Ciências Biomédicas Abel Salazar, Universidade do Porto, R. de Jorge Viterbo Ferreira, 228, 4050-313 Porto, Portugal. Electronic address: apego@i3s.up.pt.

Originally published in *J Pharm Sci.* 2020 Jan 11. pii: S0022-3549(20)30012-5. doi: 10.1016/j.xphs.2020.01.007.

INSTITUTO
DE INVESTIGAÇÃO
E INOVAÇÃO
EM SAÚDE
UNIVERSIDADE
DO PORTO

Rua Alfredo Allen, 208
4200-135 Porto
Portugal
+351 220 408 800
info@i3s.up.pt
www.i3s.up.pt

Version: Postprint (identical content as published paper) This is a self-archived document from i3S – Instituto de Investigação e Inovação em Saúde in the University of Porto Open Repository For Open Access to more of our publications, please visit <http://repositorio-aberto.up.pt/>

ABSTRACT

Current treatment options for bone-related disorders rely on a systemic administration of therapeutic agents that possess low solubility and intracellular bioavailability, as well as a high pharmacokinetic variability, which in turn lead to major off-target side effects. Hence, there is an unmet need of developing drug delivery systems that can improve the clinical efficacy of such therapeutic agents. Nano-particle delivery systems might serve as promising carriers of hydrophobic molecules. Here, we propose nanoparticle-based delivery systems based on monomethoxy poly(ethylene glycol)-poly(trimethylcarbonate) (mPEG-PTMC) and poly(lactide-co-glycolide) for the intracellular controlled release of a small hydrophobic drug (dexamethasone) to osteoblast cells *in vitro*. mPEG-PTMC self-assembles into stable nanoparticles in the absence of surfactant and shows a greater entrapment capacity of dexamethasone, while assuring bioactivity in MC3T3-E1 and bone marrow stromal cells cultured under apoptotic and osteogenic conditions, respectively. The mPEG-PTMC nanoparticles represent a potential vector for the intracellular delivery of hydrophobic drugs in the framework of bone-related diseases.

Keywords: nanomedicine; nanoparticles; polymeric drug delivery systems; biodegradable polymers; poorly water-soluble drug; polyglycolic acid (PLGA)

Background

Bone disorders comprise a wide variety of skeletal-related diseases, including the metabolic bone loss and inflammatory degenerative diseases, bone tumors, large bone defects, among others.¹ In the clinics, the current treatment options rely, mostly, on the systemic administration or local synovial injection of potent therapeutic drugs, which are commonly synthetic agents with hydrophobic properties.^{2, 3, 4} Owing to a poor drug solubility, low bioavailability and pharmacokinetic variability, these drugs are used at high concentrations leading to the occurrence of major off-target side effects.¹

To overcome these caveats, nanoparticle-based drug delivery systems have been put forward as promising vehicles for the delivery of hydrophobic molecules to increase the clinical efficacy of these drugs in stimulating bone regeneration, while diminishing the incidence of adverse off-target side effects.^{5,6} A wide variety of nanoparticles have been reported for the delivery of hydrophobic drugs, including liposomes,⁷ dendrimers,⁸ hydroxyapatite-based nanoparticles,⁹ and natural/synthetic polymers.^{10, 11, 12, 13} Among synthetic polymers, monomethoxy poly(ethylene glycol)-poly(trimethyl carbonate) (mPEG-PTMC) owns properties that makes it a potential candidate as a carrier of hydrophobic drugs.^{14,15} mPEG-PTMC is an amphiphilic copolymer formed by the hydrophobic PTMC, which undergoes enzymatic degradation *in vivo* without the formation of acidic compounds,^{16,17} and mPEG that confers an hydrophilic character to the copolymer and contributes to the stabilization of self-assembled mPEG-PTMC nanoparticles in an aqueous environment. Poly(lactide-co-glycolide) (PLGA) is one of the extensively studied biomaterials for drug delivery, and it has already been approved by the U.S. Food and Drug Administration in a variety of drug delivery applications. Indeed, PLGA is a polymeric carrier with biodegradable and biocompatible properties, and exhibits a wide range of possible degradation times and tunable physical properties.¹⁸

Specifically in the context of bone-related therapies, biodegradable polymeric nanoparticles were shown to be able to carry and deliver in a controlled manner relevant hydrophobic molecules with a supportive role in bone regeneration, such as BMPs,^{10,11,19} antibiotics,²⁰ and glucocorticoids (GCs).²¹ Dexamethasone (DEX) is a synthetic hydrophobic GC with a therapeutic potential exploited to treat several autoimmune and inflammatory conditions.^{4,22} Importantly, DEX has also been shown to play a dual regulatory role in bone metabolism, arising as a promising drug candidate for bone therapy. In vitro studies demonstrated that DEX induces either inhibitory or stimulatory effects in cell growth and bone formation, which is dependent on treatment length, dosage, osteoblast maturity, and cell species/origin.^{23, 24, 25, 26, 27} It is well recognized that at high concentrations ($\geq 10^{-6}$ mol.L⁻¹) DEX triggers apoptosis of osteoprogenitor cells and bone resorption,^{23,26} whereas at lower concentrations ($\leq 10^{-7}$ mol.L⁻¹), DEX is able to trigger osteoblast differentiation promoting the expression of osteoblastic phenotypic markers and mineralization.^{28,29} Thus, DEX arises as a promising drug model to evaluate nanoparticle delivery systems for the release of hydrophobic therapeutic drugs in bone therapies.

Here, we proposed to develop a delivery system based on mPEG-PTMC for the controlled release of DEX and compare mPEG-PTMC to the well-established PLGA polymeric nanoparticle systems. In vitro studies were conducted to evaluate the biofunctionality of the developed DEX-loaded nanoparticles in modulating osteoblast activity and differentiation under apoptotic and osteogenic conditions for bone therapies. The amphiphilic mPEG-PTMC nanoparticles appear as a promising vehicle to deliver therapeutic hydrophobic molecules in the context of bone repair, and by combining mPEG-PTMC nanoparticles with an injectable hydrogel, we could potentially replace implantation surgery with a minimal injection at the injured site.³⁰ In addition, the combination of a nanoparticle-hydrogel system offers a more controlled drug release profile and the hydrogel would provide a three-dimensional environment conducive to support new bone growth.³⁰

Experimental Section

Materials

Unless mentioned, all reagents used were supplied by Sigma-Aldrich. PLGA (molecular ratio 50:50) was used as received. mPEG-PTMC was synthesized by ring-opening polymerization, as previously described³¹ (Supporting Information). Both polymers were characterized by proton nuclear magnetic resonance (¹H-NMR, Bruker Avance III 400 Hz) (Figs. S1 and S2, Table S1).

Nanoparticle Preparation and Characterization

Nanoparticles were prepared using the salting-out method following a protocol adapted from Zhang et al.³¹ Briefly, a tetrahydrofuran (THF; Fluka) solution (3 mL) containing different polymer concentrations, ranging from 1% to 5% (w/v), was emulsified in an aqueous solution (5.45 mL) under mechanical stirring (29,900 rpm, Homogenizer VWR VDI 12) for 40 s. The aqueous phase contained 60% (w/v) of magnesium chloride hexahydrate (MgCl₂.6H₂O; Merck) and variable amounts of poly(vinyl alcohol) (PVA, 80% hydrolyzed, molecular weight of 9000-10,000 g mol⁻¹) ranging from 2% to 6% (w/v). After the formation of the oil-in-water emulsion, pure water (Synergy Ultrapure

Water Systems, Millipore®) (5.45 mL) was added under stirring for 30 s to promote the diffusion of the solvent into the aqueous phase and the formation of the nanoparticles. Nanoparticles from mPEG-PTMC were prepared without the use of any stabilizer. mPEG-PTMC and PLGA nanoparticles were centrifuged for 30 min at 20°C at 20,800x and 5200x g, respectively. The supernatant was removed, and mPEG-PTMC and PLGA nanoparticle suspensions were redispersed in an equal volume of pure water and 0.125% (w/v) PVA aqueous solution, respectively. Purified nanoparticle solutions were frozen at -80°C overnight and freeze-dried under vacuum (Freeze Dryer FreeZone 2.5 Plus) for 2-3 days. Sucrose (AppliChem) or glucose (BD Aristar) was added to the suspension before freezing. The freeze-dried nanoparticles were resuspended in pure water. The nanoparticle recovery yield (after preparation, purification and freeze-drying) was determined to be 70.7% and 71.4% for mPEG-PTMC and PLGA nanoparticles, respectively. Nanoparticle size, polydispersity index (PDI) and zeta potential were determined by using dynamic light scattering (Zetasizer Nano ZS, Malvern Instruments). All measurements were performed in triplicate at 25°C.

Drug Loading and Release Profile

Nanoparticles loaded with DEX were prepared, purified, and freeze-dried as described previously, starting from a polymer solution in THF containing 1% (w/v) of DEX. The loading of DEX into the nanoparticles was determined by ¹H-NMR. DEX-loaded mPEG-PTMC and PLGA nanoparticles were dissolved in deuterated dimethyl sulfoxide. Drug loading was calculated from the integral of DEX peaks (1H, δ = 7.3-7.28 ppm; 1H, δ = 6.23-6.20 ppm; 1H, δ = 6.00 ppm) and mPEG-PTMC peak (4H, δ = 4.14-4.11 ppm) or PLGA integral (2H, δ = 4.8-4.9 ppm). DEX release was evaluated by dispersing the nanoparticles in water or in PBS pH 7.4 at 37°C. The loaded nanoparticles were redispersed at a known concentration and transferred to a dialysis bag (Spectra/Por® Dialysis Membrane, MWCO 8000). Under sink conditions, a sample of 1.5 mL of medium was collected and the released DEX was quantified by UV-Vis spectrometry at 238 nm (Lambda 35 UV/Vis spectrometer, PerkinElmer).

Cell Culture

MC₃T₃-E1 calvaria preosteoblast cells, obtained from the European Collection of Cell Cultures, were cultured in complete α -modified minimum essential medium (α -MEM, Gibco) supplemented with 10% (v/v) heat inactivated fetal bovine serum (Gibco) and 1% (v/v) penicillin/streptomycin (P/S, Gibco). Cells were maintained at 37°C in a humidified atmosphere of 5% CO₂ and the medium refreshed every 2-3 days. Primary bone marrow stromal cells (BMSCs) were obtained from 8-week-old C₅₇BL/6 male mice, as previously described.³² Briefly, mice were sacrificed by CO₂ asphyxiation, and BMSCs were flushed out from bone femurs and tibias with complete α -MEM. Cells were seeded and allowed to grow for 7 days. Medium was replaced every 3 days. MC₃T₃-E1 and BMSCs were harvested at preconfluence using a trypsin solution, and cell viability was assessed by the trypan blue exclusion assay. Subsequently, the MC₃T₃-E1 and BMSCs were plated at 1×10^4 and 2×10^4 viable cells per cm², respectively. Cells were left undisturbed in the incubator, and medium was replenished after 24 h. One hour later, the nonconfluent cells were treated with DEX-loaded or -unloaded nanoparticles, and DEX in solution at 10^{-6} mol.L⁻¹ or 10^{-7} mol.L⁻¹ as positive controls, in case of apoptotic²³ or osteogenic²⁹ conditions, respectively. At the time of medium change, half of the volume was removed and fresh complete α -MEM was added to the cultured cells.

Cytotoxicity Assays

Cell viability was evaluated by Live/Dead assay. At 12-, 24-, and 48-h after treatment with the nanoparticles, the culture medium was removed, and the cell washed with PBS. Then, cells were treated with Calcein-AM (Molecular Probes®, 1 µg.mL⁻¹ in PBS) for 20 min at 37°C, washed twice with PBS, and treated with propidium iodide (Molecular Probes®, 10 µg.mL⁻¹ in PBS) for 5 min. After incubation with propidium iodide, the cells were washed again with PBS twice and complete medium was added to the wells. Samples were observed in an inverted epifluorescence microscopy (Zeiss Axiovert 200M, Carl Zeiss) equipped with AxioCam HR, and images analyzed using AxioVision Rel. 4.8 software.

Metabolic activity was quantified by 3-(4,5-dimethylthiazol-2-yl)-2,5-diphenyltetrazolium bromide (MTT) assay. Briefly, cells were incubated with complete α-MEM supplemented with 10% (v/v) of MTT solution at 5 mg.mL⁻¹. After 4 h, the supernatant was carefully removed, and the remaining crystals were dissolved in dimethyl sulfoxide. The well-plate was agitated for 5 min in an orbital shaker, and then absorbance was measured at 540 nm in a plate reader spectrophotometer (BioTek Plate Reader, Synergy MX).

Alkaline Phosphatase (ALP) Activity Assay

For ALP activity, cells were lysed in 1% (v/v) Triton X-100 in PBS and ALP activity was measured by incubating the lysates with an alkaline buffer (pH 10) containing 6 mmol.L⁻¹ p-nitrophenyl phosphate as substrate and 4 mmol.L⁻¹ MgCl₂ for 1 h at 37°C. Absorbance was measured at 405 nm and compared to a p-nitrophenol standard curve. ALP activity was normalized to total protein content quantified by RC-DC protein assay (Bio-Rad). For a ALP staining, cells were fixed in 4% (w/v) paraformaldehyde (Merck), washed with water, and then incubated with Naphtol AS-MX phosphate/Fast Violet B Salt in a ratio of 1:25 at RT. Cells were washed with water and allowed to air-dry before being imaged under a stereomicroscope system (Olympus SZX10, digital camera DP21).

Mineralization Assay

Calcium deposition was determined using a quantitative Alizarin Red S staining. BMSCs were fixed in ice-cold 70% (v/v) ethanol and allowed to air-dry. Subsequently, ethanol-fixed cells and matrix were stained for 15 min with a 2% (w/v) Alizarin Red S solution (pH 4.2) at RT, and extensively washed with water. Representative images were taken using a stereomicroscope system. Bound stain was then eluted with 10% (w/v) cetylpyridinium chloride and quantified by measuring the absorbance at 570 nm. Amount of calcium deposition was quantified by comparison to an Alizarin Red standard curve.

Osteocalcin Enzyme Immune Assay

Osteocalcin levels were determined by using a Mouse Gla-Osteocalcin High Sensitive Kit, according to the manufacturer's instructions (Takara Bio Inc.). Supernatant osteocalcin levels were detected at 450 nm.

Nanoparticle Cellular Uptake

Fluorescent nanoparticles were prepared as described previously, except that coumarin-6 was added at 0.03% (w/v) to the organic phase instead of the drug.³³ To assess nanoparticle cellular uptake, MC₃T₃-E1 and BMSCs were incubated with coumarin 6-loaded polymeric nanoparticles for 4 and 24 h at 37°C. After the incubation time, cells were washed with PBS, fixed in 4% (w/v) paraformaldehyde, and visualized under in a confocal laser scanning microscope (Leica SP2 AOBS SE equipped with LCS 2.61 software).

Statistical Analysis

Data are depicted as the mean \pm standard deviation (SD) or percentage of control (% of CTRL). One-way ANOVA tests were used to evaluate differences between CTRL and the different groups, and between pair of groups, using GraphPad Prism 5 for Mac OS X (version 5.0a). For all experimental analyses, statistical significance was defined as $p < 0.05$.

Results

Nanoparticles Preparation and Characterization

First, the preparation of the nanoparticles was established based on the preparation of unloaded particles. To tune the nanoparticle size and PDI, the initial polymer concentration was varied. As illustrated in Figure 1a, the obtained results revealed that no major alterations were found in terms of size and PDI with the increase of polymer content. In fact, it was possible to obtain a nanoparticle average size of 100 and 250 nm for mPEG-PTMC and PLGA, respectively. In terms of PDI, nanoparticles with low polydispersity were achieved indicating that, even at a low initial polymer content, nanoparticles remain stable with no coalescence. In addition, regarding the PLGA nanoparticles, the increase of the initial stabilizer concentration (PVA) (2%-6% w/v) resulted in a decrease of size and PDI (Fig. 1b). In the preparation of the mPEG-PTMC nanoparticles, owing to mPEG, a stabilizer was not required to promote the stabilization of the nanoparticles.

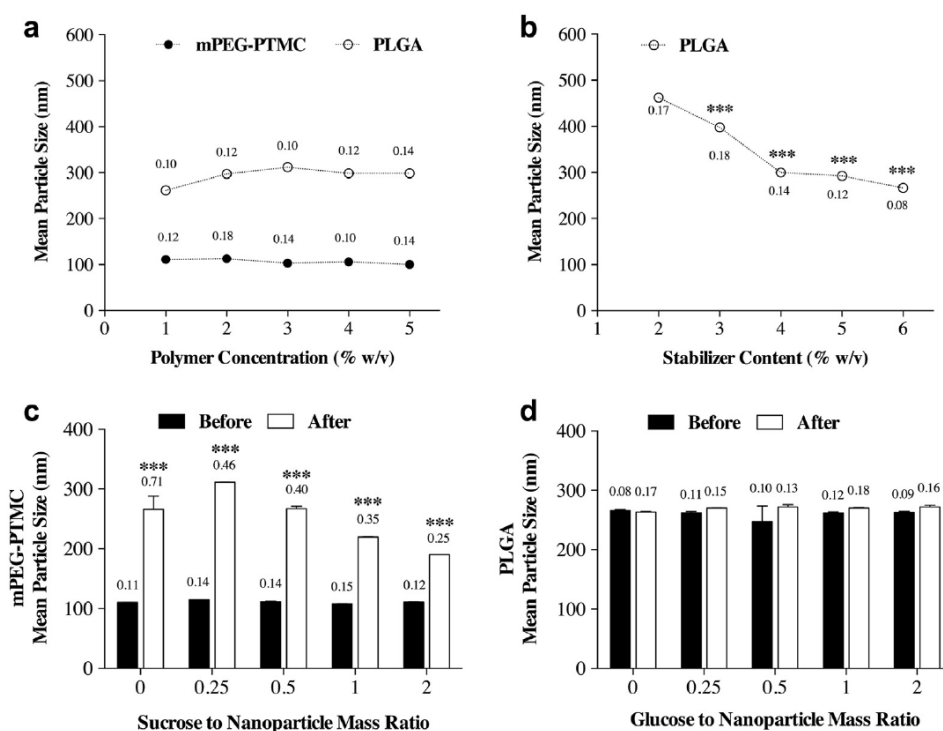


Figure 1. Characterization of mPEG-PTMC and PLGA nanoparticles. Average size and PDI of mPEG-PTMC and PLGA nanoparticles prepared with different concentrations of polymer (a) and of PLGA nanoparticles prepared by using different stabilizer concentrations (b). mPEG-PTMC (c) and PLGA (d) particle size before and after freeze-drying. Numbers in index correspond to the PDI. Mean \pm SD ($n = 9$, three independent experiments with measurements in triplicate). *** $p < 0.001$, comparing PLGA nanoparticles prepared with 2% (w/v) PVA versus other amounts of PVA. *** $p < 0.001$ different from nanoparticle size before freeze-drying.

As storage of nanoparticles in suspension presents drawbacks from an application point of view,³⁴ after preparation, both nanoparticles were freeze-dried. After freeze-drying, mPEG-PTMC exhibited significant nanoparticle aggregation, as indicated by the average size of ~ 250 nm and PDI of 0.71 (Fig. 1c, condition without sucrose). These nanoparticles did not resuspend in pure water, even under agitation for 3 days or sonication. To avoid nanoparticle destabilization, the effect of a range of weight ratios of sugar to particle mass was investigated. In a first attempt, a glucose solution was added to the nanoparticle suspension before freeze-drying; however, significant aggregation was still obtained for mPEG-PTMC (data not shown). Sucrose was then tested for mPEG-PTMC, and as observed on Figure 1c, the increase of sucrose to nanoparticle weight ratio resulted in a reduction of these nanoparticles aggregation as indicated by a decrease in size and PDI. At the higher ratio tested (2:1), mPEG-PTMC nanoparticles were easily resuspended with manual shaking in water, and dynamic light scattering analysis confirmed low PDI (0.25) compared to nanoparticles freeze-dried in the absence of sugar. For the PLGA nanoparticles no significant alterations were detected in size and PDI after the freeze-drying independently of the presence of a sugar or its concentration (Fig. 1d).

Drug Loading and In Vitro Drug Release Profile

The preparation of the DEX-loaded mPEG-PTMC nanoparticles was carried out by the salting-out method using previously reported optimized conditions.³¹ The achieved drug loading was found to be 12.8% (w/w), which corresponds to a loading efficiency of 67.8% (Table 1). Freeze-dried DEX-loaded mPEG-PTMC nanoparticles exhibited a size of 235.2 ± 6.7 nm and PDI of 0.5, which is in accordance with the obtained value for the freeze-dried unloaded nanoparticles. Zeta potential of the formulation was found to be -3.9 mV. Loading of DEX into PLGA nanoparticles was explored using varied polymer, drug, and stabilizer initial concentrations. Increasing the polymer (up to 5% w/v) and drug content ($>1\%$ w/v) showed no effect on the loading efficiency (data not shown). However, the reduction of the stabilizer concentration from 6% to 2% (w/v) resulted in an increase of DEX entrapment reaching a loading of 5.5% (w/v), which corresponds to an efficiency of 40.6% (Table 1). These freeze-dried nanoparticles exhibited a size of ~ 300 nm with low PDI (0.25) and zeta potential of -12.6 mV.

Table 1. Characterization of DEX-Loaded mPEG-PTMC and PLGA Nanoparticles

Nanoparticles Type	Polymer (% w/v)	Stabilizer (% w/v)	Drug (% w/v)	Loading (% w/w)	Loading Efficiency (%)	Mean Size (nm)	PDI	Zeta Potential (mV)
mPEG-PTMC	5.3	–	1.0	12.8 ± 0.4	67.8 ± 2.2	235.2 ± 6.7	0.51 ± 0.12	-3.9 ± 0.45
PLGA	2.0	2.0	1.0	5.45 ± 0.3	40.6 ± 2.2	309.4 ± 6.0	0.25 ± 0.01	-12.6 ± 0.1

Nanoparticle average size, polydispersity index (PDI), and zeta potential are represented as mean \pm SD ($n = 9$, three independent experiments with measurements in triplicate).

DEX release profile from the mPEG-PTMC and PLGA nanoparticles was also investigated in water and in PBS (pH 7.4) at 37°C (Fig. 2). During the first 8 h, DEX-loaded mPEG-PTMC nanoparticles showed a burst release of 80% and 50% in water and PBS, respectively, which was followed by a sustained release in both media. Interestingly, DEX release in PBS occurred for 12 days, whereas in water, the total amount of drug was released within 3 days (Fig. 2a). In the case of PLGA nanoparticles, a burst release of $\sim 60\%$ -80% of the total amount of DEX was observed within the first 24 h in both PBS and water (Fig. 2b). Burst release was followed by a sustained release for 8 days.

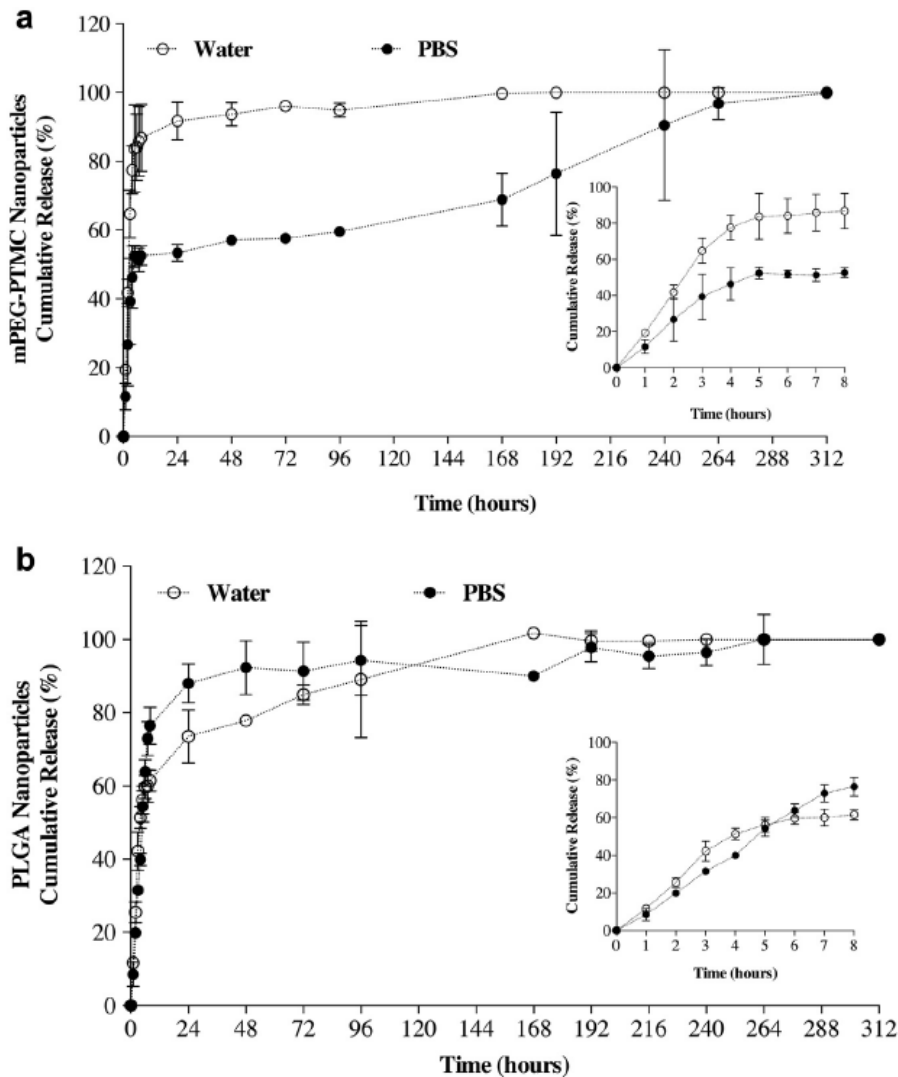


Figure 2. Release profile of DEX from mPEG-PTMC and PLGA nanoparticles. Cumulative release of DEX from mPEG-PTMC (a) and PLGA (b) in water and PBS at 37°C. Mean \pm SD (n = 6, two independent experiments with measurements in triplicate).

Biocompatibility of mPEG-PTMC and PLGA Nanoparticles

The cytotoxicity of the unloaded-nanoparticles was first tested using a pre-osteoblastic cell line, MC₃T₃-E1 cells. As shown in the Figure 3, cell metabolic activity and viability were evaluated by MTT and Live/Dead assays, respectively, after 12, 24, and 48 h in contact with increasing concentrations of unloaded mPEG-PTMC and PLGA nanoparticles. MC₃T₃-E1 cells responded in a dose-dependent manner to the increasing concentrations of mPEG-PTMC (Fig. 3a) and PLGA (Fig. 3b). MC₃T₃-E1 metabolic activity remained unaltered for 12 h when incubated with a low concentration of nanoparticles (0.004 mg.mL⁻¹) (Figs. 3a and 3b). At concentrations above 0.04 mg.mL⁻¹, a significant reduction of cell metabolic activity was observed ($p < 0.01$, $p < 0.001$, Figs. 3a and 3b) for

all time-points tested, which was more pronounced in the case of PLGA (Fig. 3b). Live/Dead assay showed that MC₃T₃-E1 cells remain viable in the presence of the nanoparticles with no major alterations in morphology by maintaining an elongated spindle shape and ability to proliferate (Figs. 3c, S3, and S4).

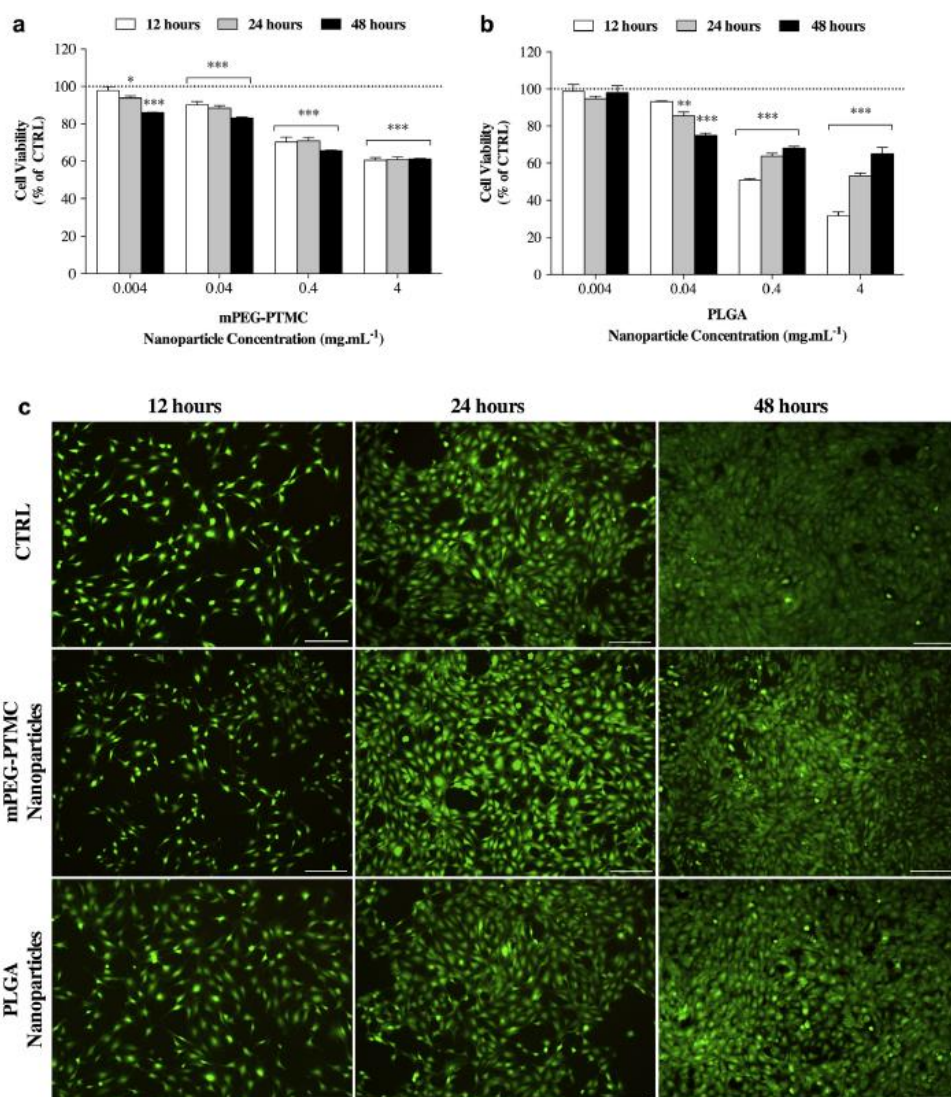


Figure 3. Biocompatibility of unloaded mPEG-PTMC and PLGA nanoparticles to MC₃T₃-E1 cells. Cell viability, as inferred from the determination of cell metabolic activity, evaluated after incubation with mPEG-PTMC (a) and PLGA (b) nanoparticles at 0.004 to 4 mg.mL⁻¹. Mean \pm SD ($n = 6$, two independent experiments in triplicate). * $p < 0.05$, ** $p < 0.01$, *** $p < 0.001$ different from CTRL (untreated cells). Cell viability was analyzed by Live/Dead assay (c). Representative images of MC₃T₃-E1 cells treated with 0.004 mg.mL⁻¹ unloaded-nanoparticles. Viable cells are stained in green and dead cells in red. Scale bar 200 μ m.

Biofunctionality of DEX-Loaded mPEG-PTMC and PLGA Nanoparticles

It is well recognized that depending on the dosage and treatment length, DEX exerts a dual regulatory role in bone metabolism. Initially, to assess the ability of our systems to release an inhibitory amount of DEX, MC₃T₃-E1 cells were cultured in contact with DEX-loaded nanoparticles that in time would release DEX in apoptotic concentrations (10^{-6} mol.L⁻¹); therefore, the amount of nanoparticles was adjusted to release a total concentration of 10^{-6} mol.L⁻¹. Metabolic activity was assessed at day 1, 3, and 7 (Fig. 4). The obtained results indicate that both unloaded nanoparticles had no significant effect on cell metabolic activity when compared to untreated cells. By contrast, after the release of apoptotic dosage of DEX, a significant decrease in cell metabolic activity was observed, which was sustained for the 7 days of culture ($p < 0.001$) for both mPEG-PTMC and PLGA nanoparticles. These results were similar to treatment with free DEX (10^{-6} mol.L⁻¹, Fig. 4).

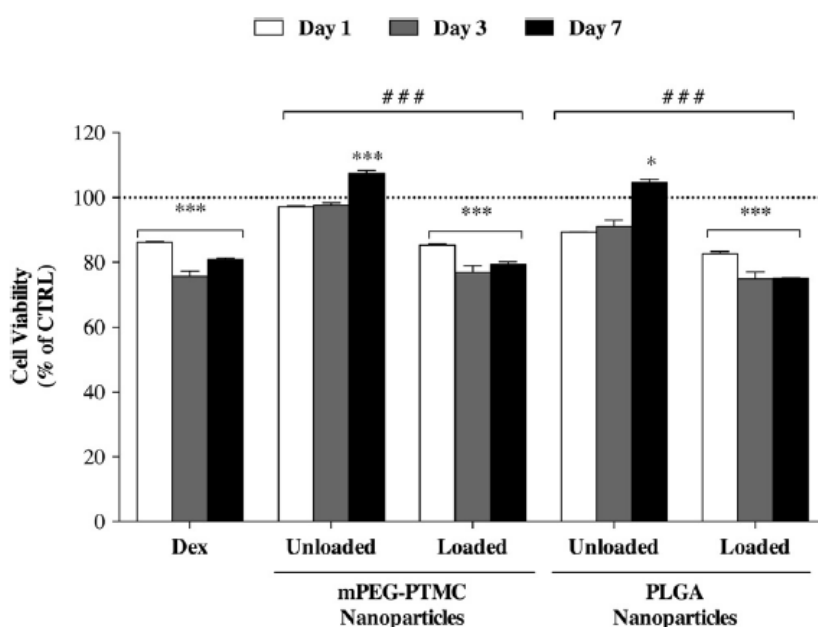


Figure 4. Inhibitory effects of the DEX released from mPEG-PTMC and PLGA nanoparticles on the cell viability of MC₃T₃-E1 cells. Cell viability was inferred from the metabolic activity determined at different time points. Free DEX (10^{-6} mol.L⁻¹) was used as a positive control. Mean \pm SD ($n = 6$, two independent experiments in triplicate). * $p < 0.05$, *** $p < 0.001$ different from CTRL. ### $p < 0.001$, loaded in relation to unloaded nanoparticles.

To further investigate the ability of the DEX-loaded nanoparticles to stimulate osteoblast differentiation, a population of osteoprogenitor cells derived from bone marrow (BMSCs), which contains a heterogeneous cell population at different stages of the differentiation, was used resembling the in vivo scenario. BMSCs were cultured for 14 days under osteogenic conditions, $50 \mu\text{g.mL}^{-1}$ ascorbic acid (Asc) and 10mmol.L^{-1} β -glycerophosphate (β -Gly), in the presence or absence of unloaded and DEX-loaded nanoparticles. In this case, the mass of the DEX-loaded nanoparticles was adjusted to obtain a controlled release of an osteogenic concentration of DEX. As a first measurement outcome, the cell metabolic activity of BMSCs was analyzed along the course of

culture (Fig. 5). Although no differences could be observed between treatments on days 3 and 7 of differentiation, free DEX and DEX-loaded nanoparticles induced a ~ 2-fold increase in the cell metabolic activity when compared to the untreated cells ($p < 0.001$) at day 14.

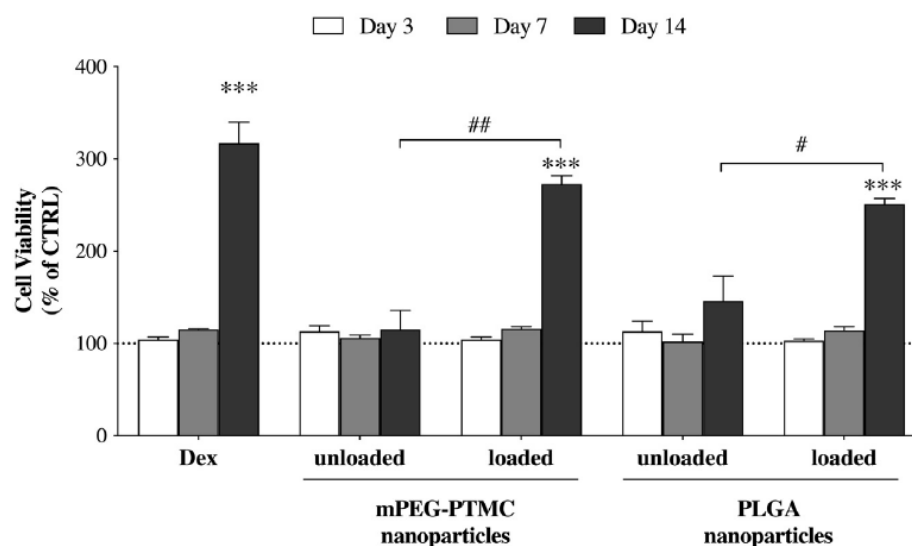


Figure 5. Stimulatory effects of DEX released from mPEG-PTMC and PLGA nanoparticles on the cell viability of BMSCs. Cell viability was inferred from the metabolic activity determined at different time points. Free DEX (10^{-7} mol.L $^{-1}$) was used as a positive control. Mean \pm SD ($n = 6$, two independent experiments in triplicate). *** $p < 0.001$ different from CTRL, # $p < 0.05$, ## $p < 0.01$ loaded in relation to unloaded nanoparticles.

The effects of DEX-loaded nanoparticles in the expression of early and late markers of bone differentiation, ALP and osteocalcin, respectively, were further assessed. As shown in Figure 6a, at day 3 of differentiation, no differences were observed between treatments. At day 7 of differentiation, a trend towards an increase in ALP activity was found in free DEX and DEX-loaded nanoparticles, which was significant for mPEG-PTMC-loaded nanoparticles comparing to untreated cells ($p < 0.05$). These results were confirmed by ALP cytochemical staining depicted by representative light microscopy images in Figure 6b. Osteogenic stimuli of DEX-loaded nanoparticles on later stages of osteoblast differentiation were assessed by quantification of the levels of osteocalcin in the media at day 14 (Fig. 6c). As anticipated, DEX released from both mPEG-PTMC and PLGA nanoparticles triggered an increase of the osteocalcin levels ($p < 0.001$, comparing loaded nanoparticles to untreated cells) comparable to the effect of free DEX. These effects were significantly higher than unloaded nanoparticles ($p < 0.001$, when comparing DEX-loaded to -unloaded nanoparticles).

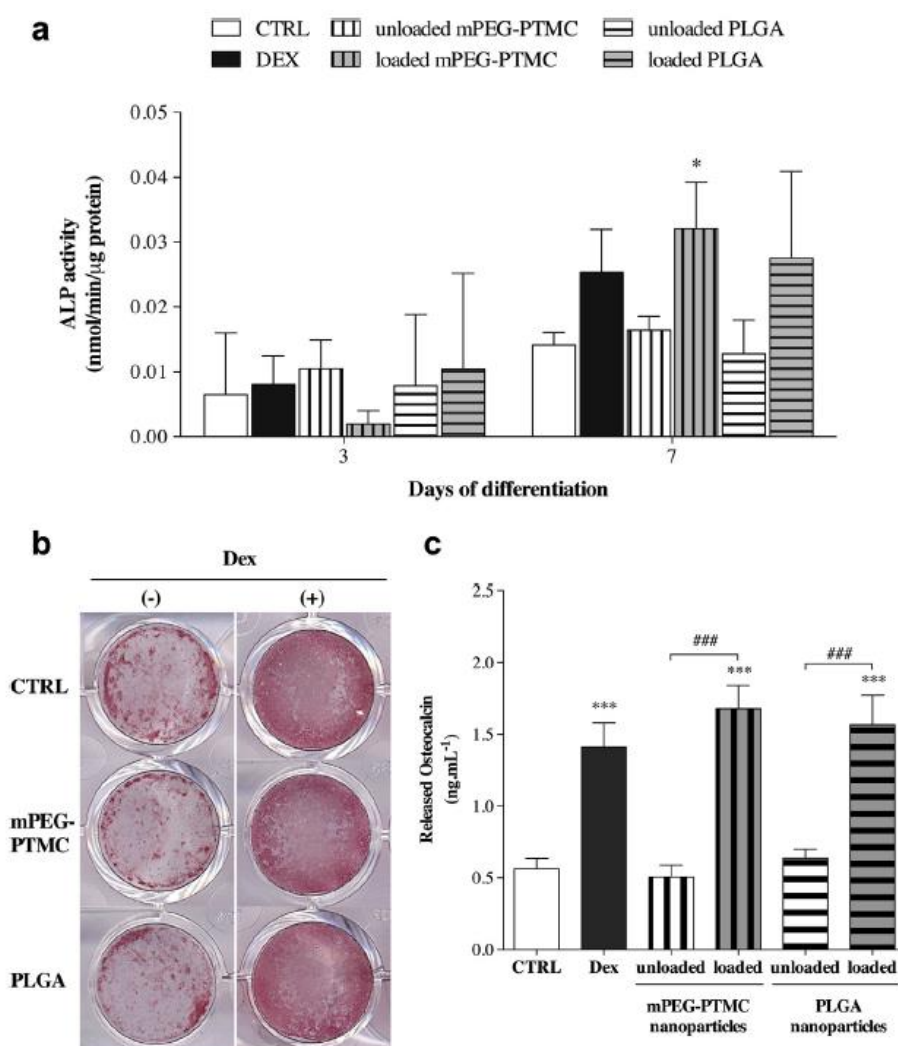


Figure 6. DEX-loaded mPEG-PTMC and PLGA nanoparticles effects on the early and late stages of osteoblast differentiation. ALP activity (nmol/min/ μ g protein) in BMSCs treated with nanoparticles loaded with an osteogenic amount of DEX (a). Representative images of ALP-stained cells after 7 days of osteogenic differentiation (b). Osteocalcin expression in the BMSCs following 14 days under differentiation in the presence/absence of unloaded and DEX-loaded nanoparticles (c). Released osteocalcin ($\text{ng}\cdot\text{mL}^{-1}$) values expressed as mean \pm SD ($n = 6$, two independent experiments in triplicate). * $p < 0.05$, *** $p < 0.001$ different from CTRL, ### $p < 0.001$ loaded in relation to unloaded nanoparticles.

In addition, calcium deposit and cell calcification were also determined in BMSCs treated with these 2 polymeric nanoparticles. At day 7 and 14 of osteogenic differentiation, BMSCs were stained using Alizarin Red S to assess matrix mineralization (Figs. 7a and 7b). As illustrated in Figure 7a, within 7 days of culture, a trend toward the increase in calcium deposition was observed for free DEX and DEX-loaded nanoparticles. However, at this time-point, no statistical significance was found in the

tested conditions except for free DEX at 10^{-7} mol.L $^{-1}$ ($p < 0.05$, when comparing free DEX to untreated cells). On day 14, calcium deposition levels were significantly higher in cells treated with DEX-loaded nanoparticles ($p < 0.001$), when compared to untreated cells. As observed for previous osteogenic markers (Fig. 6), DEX-loaded nanoparticles show significantly greater levels of Alizarin Red S when compared to unloaded nanoparticles ($p < 0.001$) (Fig. 7b).

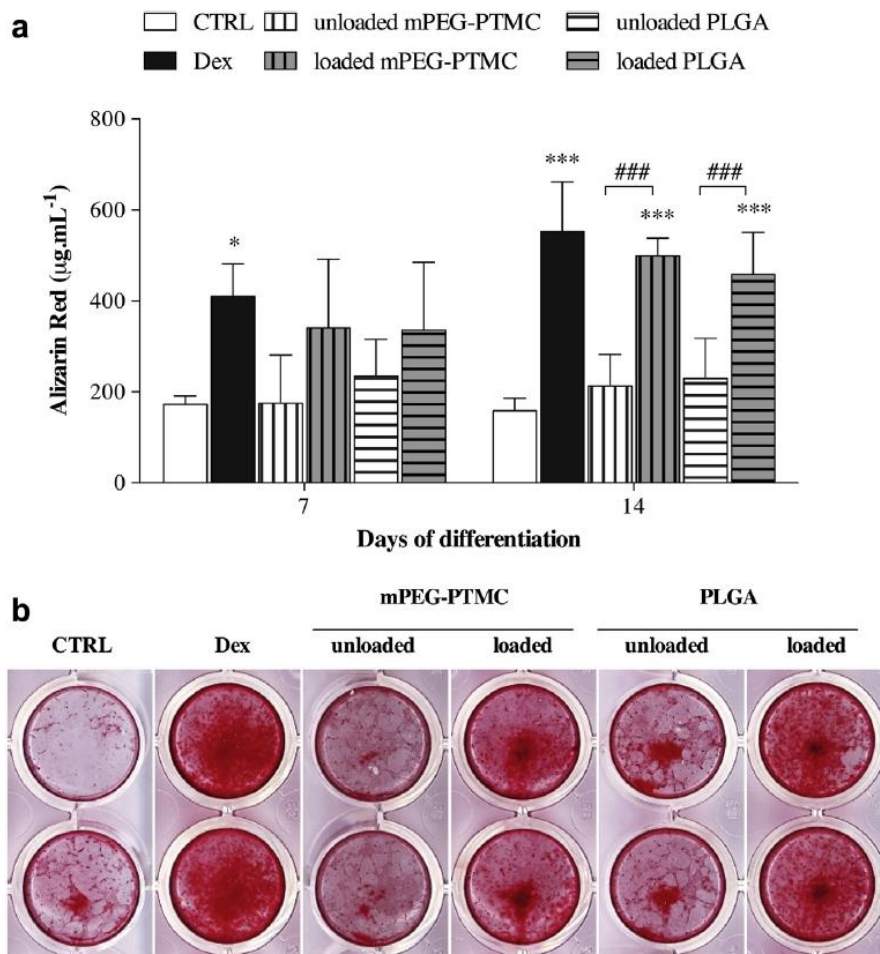


Figure 7. DEX-loaded mPEG-PTMC and PLGA nanoparticles effect in matrix mineralization. Calcium deposition in nanoparticle-treated BMSCs evaluated by quantification ($\mu\text{g.mL}^{-1}$) of Alizarin Red S (a). Representative images of the Alizarin Red S-stained cells at day 14 of differentiation (b). Mean \pm SD ($n = 6$, two independent experiments in triplicate). * $p < 0.05$, *** $p < 0.001$ different from CTRL, ### $p < 0.001$ loaded in relation to unloaded nanoparticles.

Cellular Uptake of mPEG-PTMC and PLGA Nanoparticles

DEX is an osteogenic regulatory molecule with a high binding affinity to intracellular GC receptors.⁴ Hence, we explored the ability of the mPEG-PTMC and PLGA nanoparticles to deliver their cargo (DEX) intracellularly into bone cells, MC₃T₃-E1 and BMSCs, using coumarin-6 (a small fluorescent hydrophobic molecule) to mimic DEX. Within 4 h, both nanoparticles accumulated intracellularly as demonstrated by the green dots in the cytoplasm and vicinity of the nucleus (Fig. 8). A similar tendency was observed in MC₃T₃-E1 cells (Fig. S5).

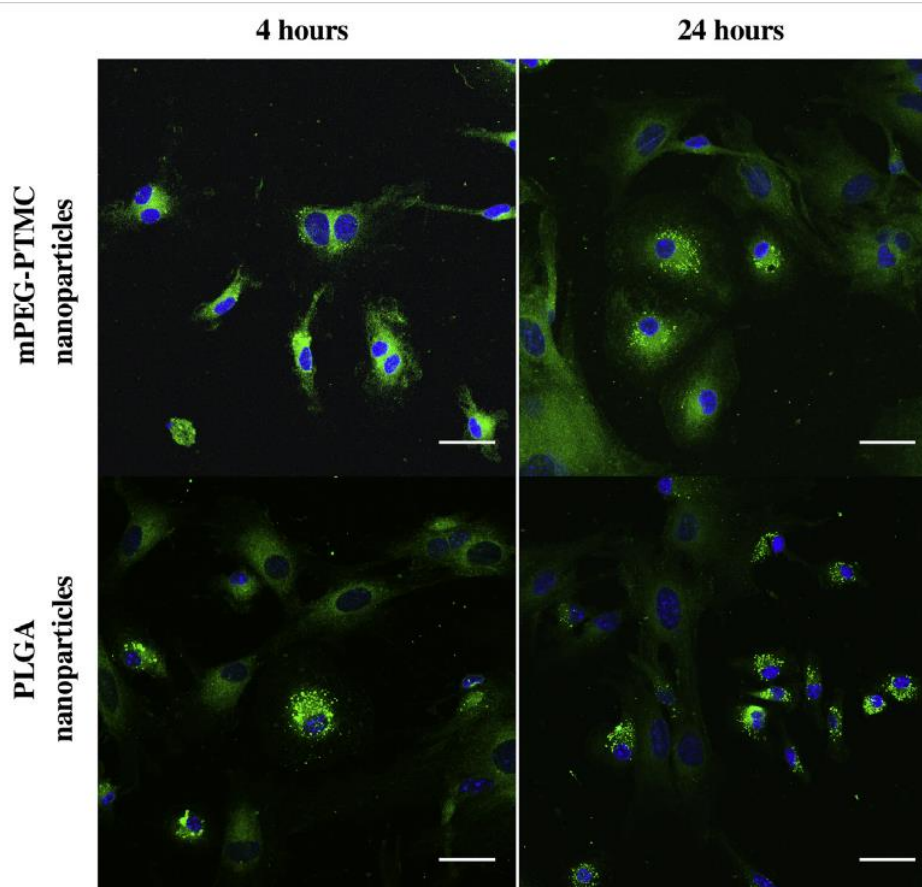


Figure 8. Cellular uptake of coumarin-6-loaded nanoparticles by BMSCs. Nanoparticles are depicted in green and the nuclei in blue. Scale bar 100 μ m.

Discussion

In this study, we have reported the development of a nanoparticle-based drug delivery system for controlled release of hydrophobic molecules known to modulate bone metabolism as a therapeutic formulation for the treatment of bone-related disorders. mPEG-PTMC-based nanoparticles were prepared using a salting-out method, loaded with DEX, and studied in vitro to assess their biofunctionality in osteoprogenitor cells. Alongside, mPEG-PTMC nanoparticles were compared to PLGA.

Nanoparticles were prepared by salting out, mainly, due to the simplicity of this methodology and ability to formulate monodisperse nanoparticles in a range of sizes.³⁵ mPEG-PTMC nanoparticles presented a size of ~100 nm and, as previously reported,³¹ the increase of initial polymer concentration was found to have no effect on the size of the nanoparticles. As for the PLGA, a size ranging 250-300 nm was obtained, which was also independent from the initial polymer amount. When comparing these 2 polymeric nanoparticles, PLGA nanoparticles exhibited a larger size compared to mPEG-PTMC. The differences might be explained based on the molecular weight of the polymers (12,000 vs. 40-75,000) as an increase in the polymer molecular weight leads to an increase in viscosity of the organic phase resulting in larger emulsion droplets, and consequently larger nanoparticles.^{36, 37, 38} It is worth to mention the amphiphilic nature of mPEG-PTMC that, in an aqueous environment, self-assembles into monodisperse nanoparticles without the need of a stabilizer due to the balance of hydrophobic/hydrophilic interactions. Hence, mPEG-PTMC nanoparticles consist in the assembly of the polymer presenting a hydrophilic brush of mPEG while PLGA nanoparticles are formed in the presence of a layer of surfactant, PVA, at the surface. Based on our size and PDI data, we observed that mPEG-PTMC nanoparticles remained stable, even using a smaller mPEG segment compared to the previous work from Zhang et al.³¹ Subsequently, both formulations were freeze-dried in the presence of cryoprotectants sucrose and glucose in the case of mPEG-PTMC and PLGA, respectively.^{39,40} The rationale for freeze-drying with sugars is that the glassy matrix of the sugars formed during the process prevents agglomeration and protects these particles from the mechanical stress induced by ice crystals that are formed in the freezing step, and also from the destabilization caused by the drying step of freeze-drying. In the case of mPEG-PTMC nanoparticles, the hydrophilic mPEG segment might be difficult for the removal of the adsorbed water in the drying step leading to irreversible aggregation. Sucrose was found to be efficient in preventing aggregation of mPEG-PTMC nanoparticles, possibly, due to the arrangement of sucrose into a more complex glassy matrix around the nanoparticles during freeze-drying.⁴¹ For PLGA nanoparticles, nonsignificant marginal alterations of particle size and PDI were observed when these nanoparticles were resuspended after freeze-drying. However, with the addition of glucose in a ratio of 2:1, the nanoparticles were more easily resuspended in water.

The entrapment of DEX within the mPEG-PTMC and PLGA nanoparticles was explored using the salting-out method. Both DEX-loaded nanoparticles revealed an average size and PDI similar to those of unloaded nanoparticles.^{31,42} Although the achieved loading efficiency for PLGA nanoparticles was relatively low (40.6%), this value is higher than previously reported for PLGA.⁴³ Using optimized parameters described by Zhang et al.,³¹ the obtained DEX loading efficiency into mPEG-PTMC was slightly lower (70%) than previously described (88.1%).³¹ Yet, mPEG-PTMC was found to entrap significant higher DEX amounts, which is possibly due to the hydrophobic interactions between PTMC and DEX during the self-assembly into nanoparticles.

In drug delivery, the kinetics of controlled drug release is a critical point to address, thus the DEX release profile from mPEG-PTMC and PLGA was investigated in water and PBS at pH 7.4. The obtained mPEG-PTMC nanoparticles revealed a faster release profile than the nanoparticles described by Zhang et al.,³¹ which might be explained by the difference in the copolymer molecular weight. Still, the DEX release in PBS spanned a period of 12 days. Interestingly, for the mPEG-PTMC nanoparticles, a significant difference was observed in the release profile of DEX in water and PBS at pH 7.4, with a slower release being observed in the PBS. The slow release profile in PBS is, possibly, due to an effect of the salts on the diffusion of the drug through the mPEG. Comparing mPEG-PTMC to PLGA, mPEG is a more hydrophilic copolymer and consequently more water and salts adsorb at the surface. The drug kinetic from polymeric nanoparticles is affected by salts in the surrounding medium by driving osmolality.⁴⁴ Thus, higher adsorption of salts at the hydrophilic brush of mPEG might change diffusion of DEX from the nanoparticles explaining the slower release profile in mPEG-PTMC in PBS. Based on the release kinetics, one can anticipate that the release of DEX from these 2 nanoparticles is driven by diffusion of the drug without a significant degradation of the polymers.³¹ However, in vivo studies will be important to further define the release profile of DEX from both nanoparticles. While PLGA degrades by hydrolysis of ester linkages through bulk erosion,⁴⁵ PTMC degrades by surface erosion with involvement of enzymes.^{16,17} Although the mPEG-PTMC degradation is yet to be studied in physiologic conditions, the degradation of the mPEG-PTMC is expected to be altered in the presence of enzymes.¹⁷

To assess the potential of mPEG-PTMC and PLGA nanoparticles in the treatment of bone-related diseases, polymeric nanoparticles were tested in contact with osteoblasts and osteoprogenitor cells in 2 scenarios: at high concentrations of DEX (10^{-6} mol.L⁻¹) to trigger apoptosis and a low concentration of DEX (10^{-7} mol.L⁻¹) to stimulate differentiation of osteoblasts. At the high concentration of DEX, mPEG-PTMC and PLGA nanoparticles were able to decrease the metabolic activity of MC₃T₃-E1 by ~ 20% for 7 days. DEX-triggered inhibition in osteoblast activity might be related to osteoblast apoptosis, as described previously when in contact with a high dose of DEX.⁴⁶ To support this, previous studies verified that DEX (10^{-6} mol.L⁻¹) induces apoptosis of osteoblastic MC₃T₃-E1 cells through the upregulation of Bcl-2 family proteins,²³ and activation of glycogen synthase kinase β 3 and p-38-mitogen-activated protein kinase.⁴⁷ Delivery of a lower concentration of DEX (10^{-7} mol.L⁻¹) promoted osteoblast differentiation and matrix mineralization. It has been stated that, in vitro osteogenic differentiation of BMSCs is under the concomitant influence of DEX, Asc, and β -Gly.^{32,48} Treatment of BMSCs with DEX-loaded mPEG-PTMC and PLGA nanoparticles stimulate the expression of osteoblast differentiation markers including ALP and osteocalcin.^{26,29} Contrary to Asc and β -Gly, DEX is a crucial stimulatory factor for the final step of in vitro mineralization.⁴⁸ We have observed that delivery of DEX by both nanoparticles increased deposition of calcium in the BMSCs-expressing matrix at day 14 of differentiation, in accordance with previous data.²⁹ Altogether, our results show that the polymeric systems are potential formulations for the treatment of bone-related diseases in which a balance between bone formation and resorption is compromised, that is, osteoporosis/osteopetrosis.⁴⁹

The cellular effects of DEX are facilitated through the activation of intracellularly-localized receptors.⁴ In both cases, mPEG-PTMC and PLGA nanoparticles are able to cross the cell membrane and accumulate in the cytoplasm of MC₃T₃-E1 and BMSCs in a short time indicating that the developed nanoparticle-delivery systems improve the intracellular delivery of DEX. These results bring new insights into the use of mPEG-PTMC and PLGA nanoparticles in intracellular delivery of

hydrophobic drugs that are known to trigger downstream signaling cascades involved in complex machinery regulating bone metabolism,⁵⁰ for example c-Src kinase inhibitors.⁵¹

To summarize, we described the development of mPEG-PTMC nanoparticles for the controlled delivery of a small hydrophobic drug—DEX, and we compared the developed nanoparticles to the established Food and Drug Administration–approved PLGA. The amphiphilicity of mPEG-PTMC copolymer allowed self-assembly into monodisperse and stable nanoparticles, and the mPEG forms a hydrophilic brush at the surface of the nanoparticles, which is well recognized to prolong circulation time in vivo.⁵² Thus, mPEG-functionalized nanoparticles appear as an advantageous strategy in drug delivery over PLGA. Loading studies revealed that DEX is entrapped at higher amounts in mPEG-PTMC nanoparticles, when comparing to the PLGA, which is also beneficial by reducing the amount of formulation required to deliver needed level of drug. In addition to this, mPEG-PTMC also revealed a lower cytotoxicity in the osteoblasts when comparing to PLGA. In vitro, mPEG-PTMC nanoparticles show similar bioactivity to PLGA. Thus, mPEG-PTMC particles appears as a potential more interesting vehicle to deliver doses of DEX, or other small hydrophobic molecules, in a controlled manner to modulate the activity of osteoblasts.

Acknowledgements

The authors would like to acknowledge Centro de Materiais da Universidade do Porto (CEMUP) for the ³¹H-NMR analysis. Confocal microscopy was conducted at the Bioimaging i3S Scientific Platform, member of the PPBI (PPBI-POCI-01-0145-FEDER-022122), with the assistance of Maria Lázaro and nanoparticle size and zeta potential determination was conducted at the Biointerfaces and Nanotechnology Scientific Platform of i3S, with the assistance of Ricardo Vidal. This work was financed by FEDER funds through the *Programa Operacional Factores de Competitividade - COMPETE* and by Portuguese funds through the *Fundação para a Ciência e a Tecnologia-FCT* (Portugal) in the framework of the financed projects PEst-C/SAU/LA0002/2013 and PTDC/BIM-MED/1047/2012; and projects NORTE-01-0145-FEDER-000008 and NORTE-01-0145-FEDER-000012, supported by Norte Portugal Regional Operational Programme (NORTE 2020), under the PORTUGAL 2020 Partnership Agreement, through the European Regional Development Fund (ERDF) and FEDER funds through the COMPETE 2020 - Operational Programme for Competitiveness and Internationalisation (POCI), Portugal 2020. DMS acknowledges FCT for her Post-doctoral fellowship (SFRH/BPD/115341/2016).

REFERENCES

1. Gu W, Wu C, Chen J, Xiao Y. Nanotechnology in the targeted drug delivery for bone diseases and bone regeneration. *Int J Nanomedicine*. 2013;8:2305-2317.
2. Francis MD, Valent DJ. Historical perspectives on the clinical development of bisphosphonates in the treatment of bone diseases. *J Musculoskelet Neuronal Interact*. 2007;7(1):2-8.
3. Bibbo C, Nelson J, Ehrlich D, Rougeux B. Bone morphogenetic proteins: indications and uses. *Clin Podiatr Med Surg*. 2015;32(1):35-43.
4. Moutsatsou P, Kassi E, Papavassiliou AG. Glucocorticoid receptor signaling in bone cells. *Trends Mol Med*. 2012;18(6):348-359.

5. Bhatt P, Lalani R, Vhora I, et al. Liposomes encapsulating native and cyclodextrin enclosed Paclitaxel: enhanced loading efficiency and its pharmacokinetic evaluation. *Int J Pharm.* 2018;536(1):95-107.
6. Pathak Y, Thassu D, Deleers M. Pharmaceutical applications of nanoparticulate drug-delivery systems. In: Pathak Y, Thassu D, Deleers M, eds. *Nanoparticulate Drug Delivery Systems*. New York, NY: Informa Healthcare; 2007:185-212.
7. Matsuo T, Sugita T, Kubo T, Yasunaga Y, Ochi M, Murakami T. Injectable magnetic liposomes as a novel carrier of recombinant human BMP-2 for bone formation in a rat bone-defect model. *J Biomed Mater Res A.* 2003;66A(4):747-754.
8. Oliveira JM, Sousa RA, Kotobuki N, et al. The osteogenic differentiation of rat bone marrow stromal cells cultured with dexamethasone-loaded carboxymethylchitosan/ poly(amidoamine) dendrimer nanoparticles. *Biomaterials.* 2009;30(5):804-813.
9. Xie G, Sun J, Zhong G, Liu C, Wei J. Hydroxyapatite nanoparticles as a controlled-release carrier of BMP-2: absorption and release kinetics in vitro. *J Mater Sci Mater Med.* 2010;21(6):1875-1880.
10. Chung Y-I, Ahn K-M, Jeon S-H, Lee S-Y, Lee J-H, Tae G. Enhanced bone regeneration with BMP-2 loaded functional nanoparticle/hydrogel complex. *J Control Release.* 2007;121(1e2):91-99.
11. Wei G, Jin Q, Giannobile WV, Ma PX. The enhancement of osteogenesis by nano-fibrous scaffolds incorporating rhBMP-7 nanospheres. *Biomaterials.* 2007;28(12):2087-2096.
12. Wang G, Siggers K, Zhang S, et al. Preparation of BMP-2 containing bovine serum albumin (BSA) nanoparticles stabilized by polymer coating. *Pharm Res.* 2008;25(12):2896-2909.
13. Zhang S, Wang G, Lin X, et al. Polyethylenimine-coated albumin nanoparticles for BMP-2 delivery. *Biotechnol Prog.* 2008;24(4):945-956.
14. Jiang X, Xin H, Sha X, et al. PEGylated poly(trimethylene carbonate) nanoparticles loaded with paclitaxel for the treatment of advanced glioma: in vitro and in vivo evaluation. *Int J Pharm.* 2011;420(2):385-394.
15. Zhao H, Wang YL, Peng JR, et al. Biodegradable self-assembled micelles based on MPEG-PTMC copolymers: an ideal drug delivery system for vincristine. *J Biomed Nanotechnol.* 2017;13(4):427-436.
16. Pêgo AP, Van Luyn MJA, Brouwer LA, et al. In vivo behavior of poly(1,3- trimethylene carbonate) and copolymers of 1,3-trimethylene carbonate with D,L-lactide or ϵ -caprolactone: degradation and tissue response. *J Biomed Mater Res A.* 2003;67A(3):1044-1054.
17. Zhang Z, Kuijer R, Bulstra SK, Grijpma DW, Feijen J. The in vivo and in vitro degradation behavior of poly(trimethylene carbonate). *Biomaterials.* 2006;27(9):1741-1748.
18. Cannizzaro SM, Langer RS. Polymeric systems for controlled drug release. *Chem Rev.* 1999;99:3181-3198.
19. Choi S-W, Kim J-H. Design of surface-modified poly(D,L-lactide-co-glycolide) nanoparticles for targeted drug delivery to bone. *J Control Release.* 2007;122(1): 24-30.
20. Pillai RR, Somayaji SN, Rabinovich M, Hudson MC, Gonsalves KE. Nafcillinloaded PLGA nanoparticles for treatment of osteomyelitis. *Biomed Mater.* 2008;3(3):034114.
21. Urbanska J, Karewicz A, Nowakowska M. Polymeric delivery systems for dexamethasone. *Life Sci.* 2014;96(1-2):1-6.
22. Weinstein RS, Jilka RL, Parfitt AM, Manolagas SC. Inhibition of osteoblastogenesis and promotion of apoptosis of osteoblasts and osteocytes by glucocorticoids. Potential mechanisms of their deleterious effects on bone. *J Clin Invest.* 1998;102(2):274-282.
23. Espina B, Liang M, Russell RG, Hulley PA. Regulation of bcl-2 in glucocorticoid-mediated osteoblast apoptosis. *J Cell Physiol.* 2008;215(2):488-496.

24. Jager M, Fischer J, Dohrn W, et al. Dexamethasone modulates BMP-2 effects on mesenchymal stem cells in vitro. *J Orthop Res.* 2008;26(11):1440-1448.
25. Leboy PS, Beresford JN, Devlin C, Owen ME. Dexamethasone induction of osteoblast mRNAs in rat marrow stromal cell cultures. *J Cell Physiol.* 1991;146(3):370-378.
26. Ogston N, Harrison AJ, Cheung HF, Ashton BA, Hampson G. Dexamethasone and retinoic acid differentially regulate growth and differentiation in an immortalised human clonal bone marrow stromal cell line with osteoblastic characteristics. *Steroids.* 2002;67(11):895-906.
27. Smith E, Redman RA, Logg CR, Coetzee GA, Kasahara N, Frenkel B. Glucocorticoids inhibit developmental stage-specific osteoblast cell cycle. Dissociation of cyclin A-cyclin-dependent kinase 2 from E2F4-p130 complexes. *J Biol Chem.* 2000;275(26):19992-20001.
28. Song IH, Caplan AI, Dennis JE. In vitro dexamethasone pretreatment enhances bone formation of human mesenchymal stem cells in vivo. *J Orthop Res.* 2009;27(7):916-921.
29. Hong D, Chen HX, Xue Y, et al. Osteoblastogenic effects of dexamethasone through upregulation of TAZ expression in rat mesenchymal stem cells. *J Steroid Biochem Mol Biol.* 2009;116(1-2):86-92.
30. Liu M, Zeng X, Ma C, et al. Injectable hydrogels for cartilage and bone engineering. *Bone Res.* 2017;5:17014.
31. Zhang Z, Grijpma DW, Feijen J. Poly(trimethylene carbonate) and monomethoxy poly(ethylene glycol)-block-poly(trimethylene carbonate) nanoparticles for the controlled release of dexamethasone. *J Control Release.* 2006;111(3):263-270.
32. Teixeira L, Sousa DM, Nunes AF, Sousa MM, Herzog H, Lamghari M. NPY revealed as a critical modulator of osteoblast function in vitro: new insights into the role of Y1 and Y2 receptors. *J Cell Biochem.* 2009;107(5):908-916.
33. Tahara K, Miyazaki Y, Kawashima Y, Kreuter J, Yamamoto H. Brain targeting with surface-modified poly(D,L-lactic-co-glycolide acid) nanoparticles delivered via carotid artery administration. *Eur J Pharm Biopharm.* 2011;77:84-88.
34. Vauthier C, Bouchemal K. Methods for the preparation and manufacture of polymeric nanoparticles. *Pharm Res.* 2008;26(5):1025-1058.
35. Pinto Reis C, Neufeld RJ, Ribeiro AJ, Veiga F, Nanoencapsulation I. Methods for preparation of drug-loaded polymeric nanoparticles. *Nanomedicine.* 2006;2(1): 8-21.
36. Budhian A, Siegel SJ, Winey KI. Haloperidol-loaded PLGA nanoparticles: systematic study of particle size and drug content. *Int J Pharm.* 2007;336(2):367-375.
37. Konan YN, Cerny R, Favet J, Berton M, Gurny R, Allemann E. Preparation and characterization of sterile sub-200 nm meso-tetra(4-hydroxyphenyl) porphyrin-loaded nanoparticles for photodynamic therapy. *Eur J Pharm Biopharm.* 2003;55(1):115-124.
38. Mittal G, Sahana DK, Bhardwaj V, Ravi Kumar MN. Estradiol loaded PLGA nanoparticles for oral administration: effect of polymer molecular weight and copolymer composition on release behavior in vitro and in vivo. *J Control Release.* 2007;119(1):77-85.
39. Abdelwahed W, Degobert G, Stainmess S, Fessi H. Freeze-drying of nanoparticles: formulation, process and storage conditions. *Adv Drug Deliv Rev.* 2006;58:1688-1713.
40. Konan YN, Gurny R, Alleman E. Preparation and characterization of sterile and freeze-dried sub-200 nm nanoparticles. *Int J Pharm.* 2002;233:239-252.
41. Carpenter JF, Pikal MJ, Chang BS, Randolph TW. Rational design of stable lyophilized protein formulations: some practical advice. *Pharm Res.* 1997;14(8):969-975.



42. Ali H, Kalashnikova I, White MA, Sherman M, Ryttinga E. Preparation, characterization, and transport of dexamethasone-loaded polymeric nanoparticles across a human placental in vitro model. *Int J Pharm.* 2013;454(1):149-157.
43. Gómez-Gaete C, Tsapis N, Besnard M, Bochot A, Fattal E. Encapsulation of dexamethasone into biodegradable polymeric nanoparticles. *Int J Pharm.* 2007;331:153-159.
44. Kamaly N, Yameen B, Wu J, Farokhzad OC. Degradable controlled-release polymers and polymeric nanoparticles: mechanisms of controlling drug release. *Chem Rev.* 2016;116(4):2602-2663.
45. Gentile P, Chiono V, Carmagnola I, Hatton PV. An overview of poly(lactic-co-glycolic) acid (PLGA)-based biomaterials for bone tissue engineering. *Int J Mol Sci.* 2014;15(3):3640-3659.
46. Liu Y, Porta A, Peng X, et al. Prevention of glucocorticoid-induced apoptosis in osteocytes and osteoblasts by calbindin-D28k. *J Bone Miner Res.* 2004;19(3): 479-490.
47. Yun SI, Yoon HY, Jeong SY, Chung YS. Glucocorticoid induces apoptosis of osteoblast cells through the activation of glycogen synthase kinase 3beta. *J Bone Miner Metab.* 2009;27(2):140-148.
48. Langenbach F, Handschel J. Effects of dexamethasone, ascorbic acid and betaglycerophosphate on the osteogenic differentiation of stem cells in vitro. *Stem Cell Res Ther.* 2013;4(5):117.
49. Lazner F, Gowen M, Pavasovic D, Kola I. Osteopetrosis and osteoporosis: two sides of the same coin. *Hum Mol Genet.* 1999;8(10):1839-1846.
50. Tautzenberger A, Kovtun A, Ignatius A. Nanoparticles and their potential for application in bone. *Int J Nanomedicine.* 2012;7:4545-4557.
51. Araujo J, Logothetis C. Targeting Src signaling in metastatic bone disease. *Int J Cancer.* 2009;124(1):1-6.
52. Bertrand N, Grenier P, Mahmoudi M, et al. Mechanistic understanding of in vivo protein corona formation on polymeric nanoparticles and impact on pharmacokinetics. *Nat Commun.* 2017;8(1):777.